

Study on the Heteroatom Influence in Pyridine-Based Nitronyl Nitroxide Biradicals with Phenylethynyl Spacers on the Molecular Ground State

Chandrasekar Rajadurai, Anela Ivanova, Volker Enkelmann, and Martin Baumgarten*

Max-Planck-Institut für Polymerforschung, Ackermannweg 10, D-55128 Mainz, Germany

baumgart@mpip-mainz.mpg.de

Received May 7, 2003

Novel pyridine-based nitronyl nitroxide (NIT) biradicals, 3,5-bis[4-(1-oxyl-3-oxo-4,4,5,5-tetramethylimidazolin-2-yl)phenylethynyl]pyridine (**1**) and 2,6-bis[4-(1-oxyl-3-oxo-4,4,5,5-tetramethylimidazolin-2-yl)phenylethynyl]pyridine (**2**), and monoradicals, 4-(5-bromopyridine-3-ylethynyl)-1-(1-oxyl-3-oxo-4,4,5,5-tetramethylimidazolin-2-yl)benzene (**3**), 4-trimethylsilylethynyl-1-(1-oxyl-3-oxo-4,4,5,5-tetramethylimidazolin-2-yl)benzene (**4**), and 4-trimethylsilylethynyl-1-(1-oxyl-3-oxo-4,4,5,5-tetramethylimidazolin-2-yl)pyridine (**5**), were synthesized and investigated by ESR and UV-vis spectroscopy. The solution EPR measurements of the biradicals gave well-resolved, nine-line spectra with exact half line spacing as compared to monoradicals ($g_{\text{iso}} = 2.0067$) with isotropic line spacing $|a_{\text{N}}| = 7.36$ G. This indicates strong, intramolecular exchange coupling ($J \gg 7 \times 10^{-4} \text{ cm}^{-1}$; $J/a_{\text{N}} \gg 1$) of the biradicals with in the limit of EPR. The temperature dependence on the $\Delta m_s = \pm 2$ signal intensity of biradicals follow Curie behavior down to 4 K ascertaining the triplet ground state or its near-degeneracy with the singlet state. UV-vis studies of **1**–**5** show characteristic differences in the extinctions of $n-\pi^*$ transitions around 600 nm. Both biradicals **1** and **2** were crystallized in monoclinic space groups $C2/c$ and $P2_1/a$ with the intraradical distances 1.54 and 1.47 nm, respectively. Computational studies of the biradicals **1**, **2**, and 1,3-bis[4-(1-oxyl-3-oxo-4,4,5,5-tetramethylimidazolin-2-yl)phenylethynyl]benzene (**T**) were performed by the AM1/CAS(8,8) method to calculate the singlet–triplet (ΔE_{ST}) energy difference and the spin density distribution. Results show that the position of the pyridyl nitrogen in **1** and **2** in comparison with **T** does not alter the triplet ground-state spin multiplicities supporting the obtained experimental results.

Introduction

Organic high spin molecules are a topic of current interest in order to understand the magnetic interactions in and between molecules for the design and synthesis of molecular-based magnets.¹ The key in obtaining magnetic ordering is the formation of very high spin domains. This has proven to be very difficult for organic polymers, since often large number of defects^{2a–c} from incomplete radical site formation or their loss reduce their effectiveness. Thus, ordering of discrete high spin molecules through hydrogen bonding^{3a–d} or metal coordination is still a promising approach. Metal complexation can be achieved via stable radical sites themselves especially with nitroxides,⁴ nitronyl nitroxide⁵ (NIT), and imino nitroxides⁶ or combined with conjugated fragments carrying heteroatoms such as pyridine, bipyridine, terpy-

ridine, etc.⁷ For the design of high spin molecules, control of geometry and topology are crucial.⁸ The sign of molecular exchange interaction (J) can be either positive or

(1) (a) Lahti, P. M. *Magnetic Properties of Organic Materials*; Marcel Dekker: New York, 1999. (b) *Diradicals*; Borden, W. T., Ed.; John Wiley and Sons: New York, 1982. (c) Crayston, J. A.; Devine, J. N.; Walton, J. C. *Tetrahedron* **2000**, *56*, 7829–7857. (d) Dougherty, D. A. *Acc. Chem. Res.* **1991**, *24*, 88–94. (e) Baumgarten, M. *Molecular Magnets*. In *EPR of free radicals in Solids: Trends in Methods and Applications*; Lund, A., Shiotani, M., Eds.; Kluwer: Norwell, MA., 2003; Chapter 12, in press.

(2) (a) Rajca, A. *Chem. Rev.* **1994**, *94*, 871–893. (b) Rajca, A.; Wongsriratanakul, J.; Rajca, S. *Science* **2001**, *294*, 1503–1505. (c) Rajca, A. *Chem. Eur. J.* **2002**, *8*, 21, 4835–4841.

(3) (a) Romero, F. M.; Ziessel, R.; Bonnet, M.; Pontillon, Y.; Res-souche, E.; Schweizer, J.; Delley, B.; Grand, A.; Paulsen, C. *J. Am. Chem. Soc.* **2000**, *122*, 1298–1309. (b) Ferrer, J. R.; Lahti, P. M.; George, C.; Oliek, P.; Julier, M.; Palacio, F. *Chem. Mater.* **2001**, *13*, 2447–2454. (c) MasPOCH, D.; Catala, L.; Gerbier, P.; Ruiz-Molina, D.; Vidal-Gancedo, J.; Wurst, K.; Rovia, C.; Veciana, J. *Chem. Eur. J.* **2002**, *8*, 16, 3635–3645. (d) Zhang, J.; Baumgarten, M. *Chem. Phys.* **1997**, *222*, 1–7.

(4) (a) Iwahori, F.; Inoue, K.; Iwamura, H. *J. Am. Chem. Soc.* **1999**, *121*, 7264. (b) Kumagai, H.; Inoue, K. *Angew. Chem., Int. Ed.* **1999**, *38*, 1601.

(5) (a) Fettouhi, M.; Khaled, M.; Waheed, A.; Golhen, S.; Ouahab, L.; Sutter, J. P.; Kahn, O. *Inorg. Chem.* **1999**, *38* (18), 3967–3971. (b) Caneschi, A.; Gatteschi, D.; Langier, J.; Pardil, L.; Rey, P.; Zanchini, C. *Inorg. Chem.* **1998**, *37*, 2027–2032. (c) Fegy, K.; Luneau, D.; Ohm, T.; Paulsen, C.; Rey, P. *Angew. Chem., Int. Ed.* **1998**, *37* (9), 1270–1273.

(6) (a) Luneau, D.; Rey, P.; Laugier, J.; Fries, P.; Caneschi, A.; Gatteschi, D.; Sessoli, R. *J. Am. Chem. Soc.* **1991**, *113*, 1245–1251. (b) Cogne, A.; Laugier, J.; Luneau, D.; Rey, P. *Inorg. Chem.* **2000**, *39*, 5510–5514.

(7) (a) Halcrow, M. A.; Brechin, E. K.; McInnes, E. J. L.; Mabbs, F. E.; Davies, J. E. *J. Chem. Soc., Dalton Trans.* **1998**, 2477. (b) Stroh, C.; Ziessel, R. *Tetrahedron Lett.* **1999**, *40*, 4543–4596. (c) Stroh, C.; Turek, P.; Rabu, P.; Ziessel, R. *Inorg. Chem.* **2001**, *40*, 5334. (d) Romero, F. M.; Ziessel, R. *Tetrahedron Lett.* **1999**, *40*, 1895–1898. (e) Zoppellaro, G.; Ivanova, A.; Enkelmann, V.; Geies, A.; Baumgarten, M. *Polyhedron* **2003**, *22*, 2099–2110. (f) Caneschi, A.; Ferraro, F.; Gatteschi, D.; Rey, P.; Sessoli, R. *Inorg. Chem.* **1991**, *30*, 16, 3162–3166.

negative depending on the coupling unit between the radical sites and their steric demands. Most often, *m*-phenylene bridging, leading to non-Kekulé structures, have been used for high-spin ground-state formation.⁹ To obtain a ferromagnetically coupled system, apart from topology, the geometry of the molecules,¹⁰ the nature and position of the substituents,¹¹ and heteroatom influence^{12,13a} are to be considered in the design of high-spin molecules. Understanding the effect of the heteroatom position like nitrogen in the ground-state spin multiplicity is important since the role of nitrogen is pivotal for metal complexation in constructing higher dimensional magnetic architectures.

In this context, Dougherty's group^{12a} has probed the influence of heteroatom in non-Kekulé systems and reported a stable quintet ground state for a series of neutral pyridine-based tetraradicals (3,5-, 2,6-, and 2,4-isomers) generated by the photolysis of the corresponding neutral bisdiazenes. It was found that the position of the pyridyl nitrogen in all the three isomers had no influence on the ground-state spin multiplicities. Also, Lahti and co-workers^{12b} described high-spin ground states for dinitrenes attached to pyridines in the 2,6- and 2,4-positions. Interestingly, in contrast to the above reports, Takui and co-workers^{13a} examined the molecular ground state of nitronyl nitroxide biradicals substituted to 2,6- and 3,5-pyridines and reported the $S = 1$ ground state for 2,6-pyridine nitronyl nitroxide radicals based on magnetic susceptibility measurements and $S = 0$ state for the corresponding 3,5-pyridine biradicals based on EPR and magnetic susceptibility measurements. For carbene spin sources,^{13b} reverted high spin stabilities were found as compared to nitronyl nitroxide, the low spin ground state was described for 2,6-pyridine bridging and high spin quintet ground state for the 3,5-pyridine bridging, rea-

soned by opposite effects of the heteroatom locations. Wautelet et al. have reported the singlet ground state for the methyl and methoxy carrying bisimino nitroxide derivative of **T** (1,3-bis[4-(1-oxyl-3-oxo-4,4,5,5-tetramethylimidazolin-2-yl)phenylethynyl]benzene) (Figure 1). The interplay between the spin polarization and the spin delocalization (π -conjugation) mechanisms was reasoned for the observed singlet ground state.^{13c,d} Accidentally, the half field signal was not observed by EPR and no comparison with the stronger exchange coupled bisnitronyl nitroxide was made.^{13c-e}

Phenylethynyl spacers carrying nitronyl nitroxide biradicals as in **1** and **2** attached to the pyridine units without functional groups were designed in this work, to clearly deduce the influence of the pyridyl nitrogen position on the ground state spin multiplicities. Intramolecularly separated radicals, on the other hand (e.g., **1** and **2**), need strong π -conjugation for achieving a strong, intramolecular exchange interaction. In this aspect, aryethynyl units are versatile building blocks for spatially separated radicals in a molecule because of their rigid and conjugated nature.^{13f,g} Formation of alternating spin density waves along the near planar conjugated spacer is good for high spin formation. Besides using the EPR spectroscopy for studying the exchange interactions, the optical spectra in the visible range have proven valuable for the identification of the number of radicals in solution and will be described. The synthesis of high spin biradicals **1** and **2**, which are based on the types of reactions involved in the preparation of the model compounds **4** and **5**, is described (Figure 2). The basic reaction sequence involves synthesis of dialdehydes,¹⁴ followed by condensation reaction¹⁵ with 2,3-dimethyl-2,3-bis(hydroxylamino)butane, and finally oxidation using NaIO₄ under phase-transfer conditions. The detailed EPR, UV-vis, single-crystal X-ray analysis, and computational studies will also be described.

Results and Discussion

Synthesis of 1–5. The synthetic sequence toward high-spin biradicals **1** and **2** is based on the building block **8**,^{14a,b} which was prepared via Sonogashira coupling of *p*-bromobenzaldehyde with trimethylsilylacetylene (TMSA) to give **6**, followed by deprotection of the silyl group^{14c} upon stirring with K₂CO₃ in methanol under argon to give **8**. Compound **8** was used to build the dialdehydes **9** and **11** using 3,5- and 2,6-dibromopyridines in the presence of catalysts Pd(PPh₃)₂Cl₂, CuI, and Et₃N base. The cross-coupling reactions for **9** and **11** involve absolutely dry argon conditions obtained by freeze-pump-thaw cycles. This is necessary to avert homocoupling of **8** to form a dimer. The dimers become the predominant product if the oxygen is not properly excluded from the reaction vessel. Together with the dialdehydes, monocoupled products (**10** in case of reaction **f**) were also obtained.

The dialdehydes have low R_f values as compared to dimers and monocoupled products in chloroform and

(8) (a) Longuet-Higgins, H. C. *J. Chem. Phys.* **1950**, *18*, 265. (b) McConnell, H. M. *J. Chem. Phys.* **1963**, *39*, 1916. (c) Ovchinnikov, A. A. *Theor. Chim. Acta.* **1978**, *47*, 297. (d) Baumgarten, M. *Acta Chem. Scan.* **1997**, *51*, 193. (e) Nau, W. M. *Angew. Chem., Int. Ed. Engl.* **1997**, *36*, 2445.

(9) (a) Ishida, T.; Iwamura, H. *J. Am. Chem. Soc.* **1991**, *113*, 4238. (b) Kanno, F.; Inoue, K.; Koga, N.; Iwamura, H. *J. Phys. Chem.* **1997**, *97*, 13267. (c) Inoue, K.; Iwamura, H. *J. Am. Chem. Soc.* **1994**, *116*, 3173. (d) Inoue, K.; Iwamura, H. *Adv. Mater.* **1996**, *8*, 73. (e) Inoue, K.; Iwamura, H. *Angew. Chem., Int. Ed. Engl.* **1995**, *34*, 927. (f) Borden, W. T.; Iwamura, H.; Berson, J. A. *Acc. Chem. Res.* **1994**, *27*, 109. (g) Borden, W. T.; Davidson, E. R. *J. Am. Chem. Soc.* **1977**, *99*, 4587.

(10) Okada, K.; Imakura, T.; Oda, M.; Baumgarten, M. *J. Am. Chem. Soc.* **1996**, *118*, 3047.

(11) (a) Dvornitzki, M.; Chiarelli, R.; Rassat, A. *Angew. Chem., Int. Ed. Engl.* **1992**, *31*, 180. (b) Kanno, F.; Inoue, K.; Koga, N.; Iwamura, H. *J. Am. Chem. Soc.* **1993**, *115*, 847.

(12) (a) West, A. P., Jr.; Silverman, S. K.; Dougherty, D. A. *J. Am. Chem. Soc.* **1996**, *118*, 1452. (b) Chapyshev, S. V.; Walton, R.; Sanborn, J. A.; Lahti, P. M. *J. Am. Chem. Soc.* **2000**, *122*, 1580–1588. (c) Rule, M.; Matlin, A. R.; Seeger, D. E.; Hilinski, E. F.; Dougherty, D. A.; Berson, J. A. *Tetrahedron* **1982**, *38*, 787. (d) Liao, Y.; Xie, C.; Lahti, P. M.; Weber, R. T.; Jiang, J.; Barr, D. P. *J. Org. Chem.* **1999**, *64* (14), 5176–5182.

(13) (a) Shiomi, D.; Ito, K.; Nishizawa, M.; Sato, K.; Takui, T.; Itoh, K. *Synth. Met.* **1999**, *103*, 2271–2272. (b) Bae, J. Y.; Yano, M.; Sato, K.; Shiomi, D.; Takui, T.; Kinoshita, T.; Abe, K.; Itoh, K.; Hong, D. *Synth. Met.* **1999**, *103*, 2261. (c) Turek, P.; Wautelet, P.; Moigne, J. L.; Stanger, J. L.; Andre, J. J.; Bieber, A.; Rey, P.; Cian, A. D.; Fischer, J. *Mol. Cryst. Liq. Cryst.* **1995**, *272*, 99–108. (d) Wautelet, P.; Moigne, J. L.; Videva, V.; Turek, P. *J. Org. Chem.* **2003**, *68*, 8025–8036. (e) Wautelet, P.; Catala, L.; Bieber, A.; Turek, P.; Andre, J. J. *Polyhedron* **2001**, *20*, 1571–1576. (f) Catala, L.; Turek, P.; LeMoigne, J.; De Cian, A.; Kyritsakas, N. *Tetrahedron Lett.* **2000**, *41*, 1015. (g) Murata, S.; Iwamura, H. *J. Am. Chem. Soc.* **1991**, *113*, 5547. (h) Catala, L.; Moigne, J. L.; Kyritsakas, N.; Rey, P.; Novoa, J. J.; Turek, P. *Chem. Eur. J.* **2001**, *7*, 2466–2480.

(14) (a) Sonogashira, K.; Tohada, Y.; Hagihara, N. *Tetrahedron Lett.* **1975**, 4467–4470. (b) Thorand, S.; Krause, N. *J. Org. Chem.* **1998**, *63*, 8551–8553. (c) Austin, W. B.; Bilow, N.; Kelleghan, W. J.; Lau, K. S. Y. *J. Org. Chem.* **1981**, *46*, 2280–2286.

(15) Osiecki, J. H.; Ullman, E. F. *J. Am. Chem. Soc.* **1968**, *90*, 1078.

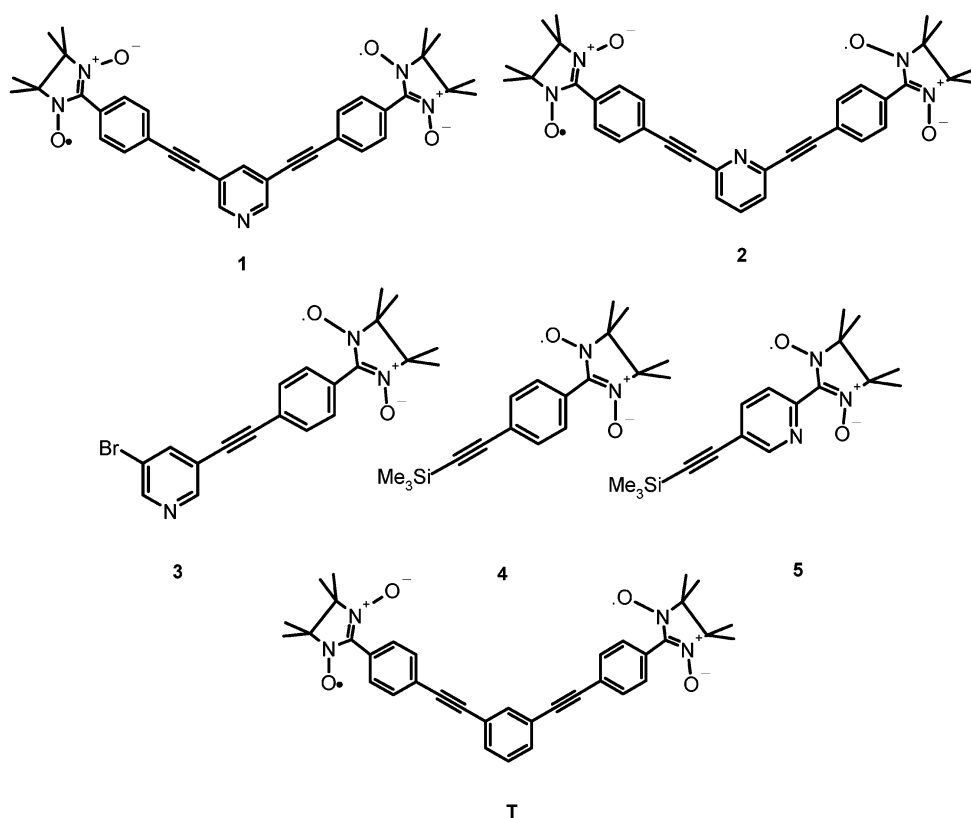


FIGURE 1. Mono- and bis(nitronyl nitroxide) radicals **1–5 T**.

dichloromethane. Purification of the dialdehydes was done by column chromatography. The condensation reactions of aldehydes (**6**, **9–11**) with 2,3-dimethyl-2,3-bis(hydroxylamino)butane were performed in MeOH with cosolvents, THF for **6**, dichloromethane for **9**, and toluene for both **10** and **11**, respectively. Mild reflux under constant argon bubbling for **9–11** and for **6** stirring for 1 day led to the precipitation of the condensation products. The oxidation reactions of the condensed products were performed in a phase-transfer solution (water/ CHCl_3) with NaIO_4 by stirring for 10 min to prevent the overoxidation of NIT to the imino nitroxides. The biradicals **1** and **2** are blue in color and are stable up to 1 year even in toluene solution. The biradicals were crystallized in toluene, and the obtained blue single crystals were used for X-ray crystal and molecular structure analysis.

Monoradical **5** was prepared in four steps. The first step involves synthesis of 2-formyl-5-bromopyridine,¹⁶ which was carried out in two steps: (1) selective monolithiation of 2,5-dibromopyridine in the 2-position to generate 5-bromo-2-lithiopyridine using *n*-BuLi (1.6 M in hexane) at $-78\text{ }^\circ\text{C}$ in toluene (50 mL for 1 g of 2,5-dibromopyridine); followed by (2) addition of dry DMF and quenching with saturated solution of NH_4Cl . The yield was up to 23% after column chromatography. The coupling reaction of the aldehyde **15** with TMSA in order to form **16** was performed via Sonogashira coupling (Figure 3). The TMSA-coupled product was obtained as sticky dark brown mass, which was difficult to purify by regular workup and column chromatography. Alternatively, direct sublimation of the dark brown mass was carried out in order to get analytically pure, light brown

crystalline powder up to 33% yield. During condensation reaction of **16** with 2,3-dimethyl-2,3-bis(hydroxylamino)butane, no precipitate was obtained after 2 days stirring in methanol. Following solvent evaporation, the obtained crude product was used for oxidation reaction with NaIO_4 in $\text{CHCl}_3/\text{water}$ to afford **5**.

Optical properties. The UV–vis spectra of the NIT radicals are very useful tools to estimate approximately the number of radical units in a single molecule based on the extinction coefficient of the $n-\pi^*$ transition in the visible range of the spectrum at $\sim 600\text{ nm}$, provided that the functionality and the backbones are quite similar (Figure 4). In this scope we have attempted to compare the extinctions ($n-\pi^*$ transition) of **4** with those of **1** and **2**. In contrast to our expectation, the biradicals **1** and **2** have extinctions of $470\text{ M}^{-1}\text{ cm}^{-1}$ and $530\text{ M}^{-1}\text{ cm}^{-1}$, respectively, which are not exactly twice as compared to the extinction of **4** which is $339\text{ M}^{-1}\text{ cm}^{-1}$ at 611 nm . The vibronic coupling pattern on the other hand is very similar for **1**, **2**, and **4**. The lowered extinctions of **1** and **2** compared to **4** may be due to the presence of pyridine unit. Indeed monoradicals **3** and **5** have extinctions of $252\text{ M}^{-1}\text{ cm}^{-1}$ at 620 nm and $266\text{ M}^{-1}\text{ cm}^{-1}$ at 581 nm (blue shifted without vibronic coupling due to loss in symmetry), respectively, which are much lower than for the benzene based monoradical **4**. The extinctions of **3** and **5** are now reasonable as compared to the doubled extinction's of **1** and **2**, proving that the pyridine unit has predominant role in lowering some of the extinction coefficient of the biradicals even in the presence of phenylethynyl spacers.

(16) Wang, X.; Rabbat, P.; O'Shea, P.; Tillyer, R.; Grabowski, E. J. J.; Reider, P. J. *Tetrahedron Lett.* **2000**, *41*, 4335–4338.

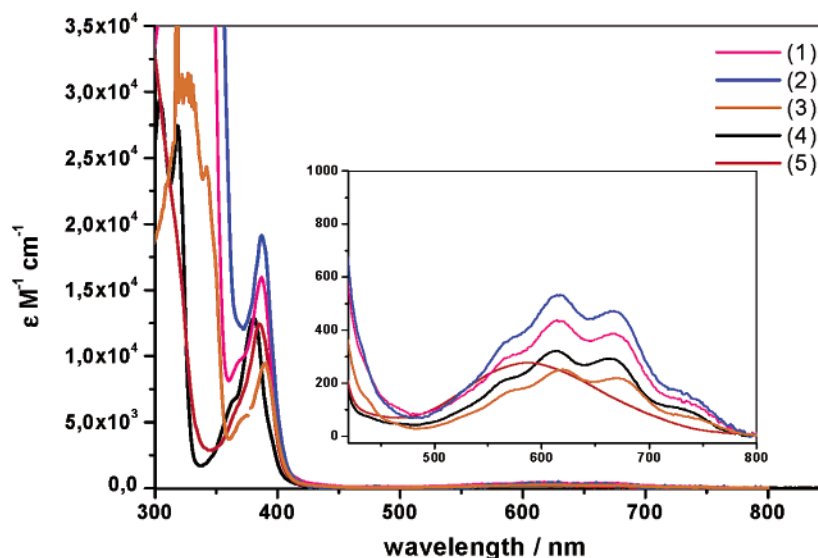


FIGURE 4. UV-vis spectra of **1–5** (in toluene), inset shows the differences of the $n-\pi^*$ transitions as molar extinction coefficients.

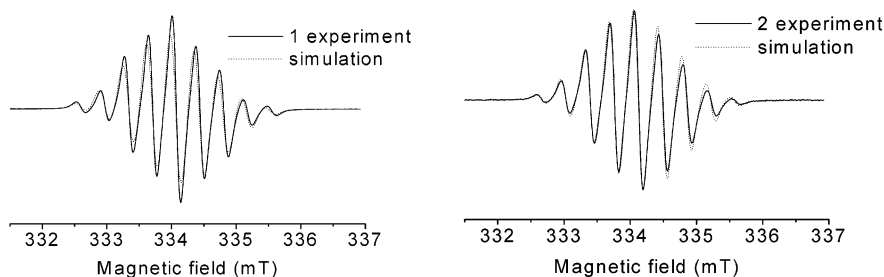


FIGURE 5. Experimental ESR spectra ($\Delta m_s = \pm 1$) of **1** and **2** in toluene ($c = 10^{-3}$ M) at 240 K (—) and their simulated spectra (⋯).

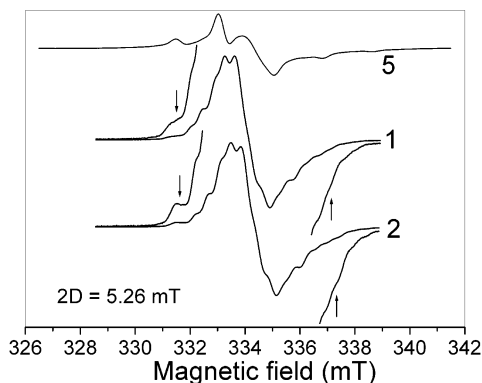


FIGURE 6. ESR spectra ($\Delta m_s = \pm 1$) of **1** and **2** in toluene glass ($c = 10^{-4}$ M) at 120 K (0.2 mW microwave power) in comparison with monoradical **5** (arrows show the enlarged outermost zfs components).

the distance vector along the i and j axis, and ρ_i and ρ_j are the spin densities on atoms i and j . In NIT the spin densities are mainly delocalized on O–N–C–N–O bonds, besides that, for extended π -conjugated systems like **1** and **2** the electron spins are delocalized along the conjugated pathways.

The approximate D values taken from the nearly symmetric fine structures of the biradicals **1** and **2** are $D \sim 0.24 \times 10^{-4}$ cm $^{-1}$. The monoradical **5** exhibits very different anisotropy with strong asymmetric spectral

pattern (Figure 6). This additionally proves that, there is no monoradical contribution in the biradicals. Based on this considerations, the derived distances for both biradicals are $r \sim 1.02$ nm.

To ascertain the intramolecular biradical nature of **1** and **2**, 10^{-3} M concentrations were used to measure (microwave power = 3.9 mW, number of scans = 10, receiver gain = 8×10^5 , modulation frequency = 100 kHz, modulation amplitude = 0.4 mT) the forbidden half field transitions ($\Delta m_s = \pm 2$) down to liquid helium temperature. The measurements were repeated at different microwave powers in order to ensure that the signals were not saturated, by plotting the observed signal intensities with respect to the square root of the microwave power used. The plot of the doubly integrated and of the peak to peak signal intensities of the $\Delta m_s = \pm 2$ signal versus inverse temperature (Figure 7) followed a Curie pattern with strong increase in signal intensity down to liquid helium temperature indicating triplet ground state or its very near degeneracy with the singlet state. Certainly the exchange coupling J cannot be very large, but a ferromagnetic exchange of $J \sim 10\text{--}15$ K is in line with the results, while an antiferro-magnetic exchange could only be as small as $|J| < 2$ K.

Molecular Structures of 1 and 2 in the Solid State. Single crystals suitable for X-ray studies were selected and the structures were determined and con-

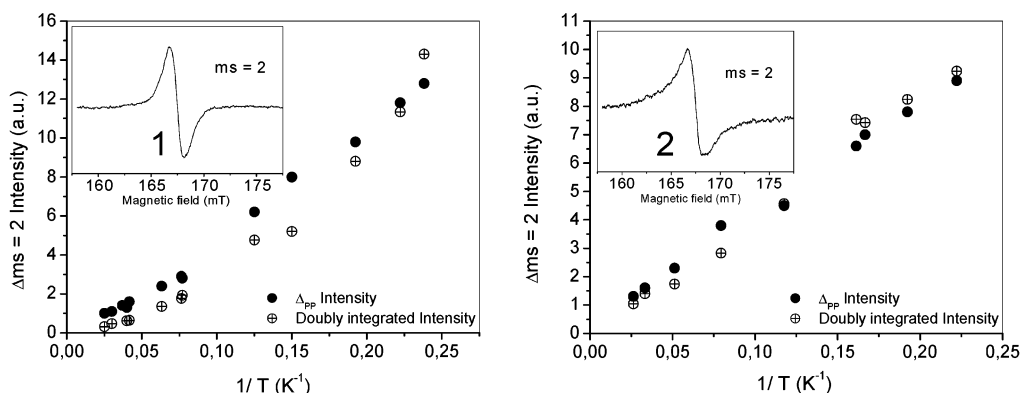


FIGURE 7. Temperature dependence of the doubly integrated signal intensities and the peak-to-peak signal intensities of the $\Delta m_s = \pm 2$ (Curie plot) transitions of **1** and **2**. The insets show the respective $\Delta m_s = \pm 2$ signal at 4.5 K.

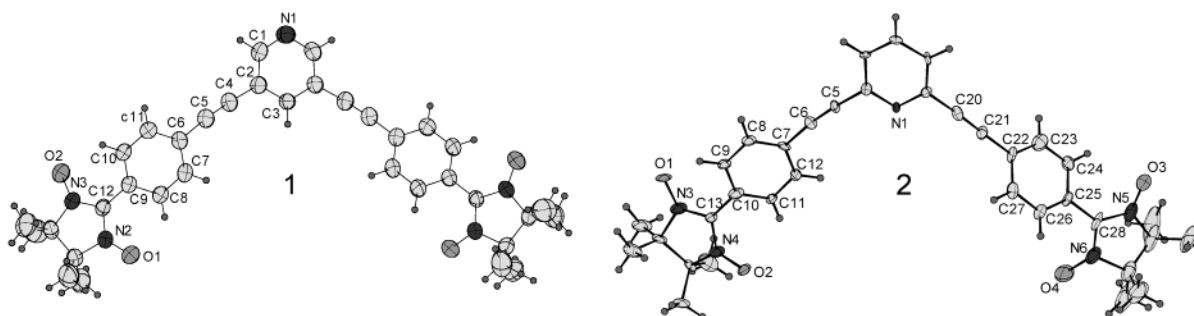


FIGURE 8. ORTEP diagrams of **1** and **2** with thermal ellipsoid plot (50% probability) with numbering scheme.

firmed with monoclinic crystal system in $C2/c$ and $P2_1/a$ space groups for **1** and **2** (with toluene molecule), respectively.

As shown in the ORTEP diagram (Figure 8), radical **1** is symmetric to the central pyridine while radical **2** is slightly distorted from symmetry. The intramolecular distance between the two radical carbon centers (O–N–C–N–O) were measured for **1** and **2**, which are 1.54 and 1.47 nm, respectively. Per unit cell four molecules of **1** and three molecules of **2** (with four toluene) were found and the molecules of **1** and **2** are packed in the c -axis. The torsional angles between the benzene ring and radical plane are 28.41° (C11–C10–C13–N4), and due to the location of toluene molecule close to the radical the plane is distorted by 33.15° (C24–C25–C28–N5) for **2**, and in **1** both arms have 21.03° (C10–C9–C12–N3). The O–N–C–N–O moiety is planar, with nearly equivalent O–N bond lengths of 1.299(1) Å (O1–N3); 1.29(1) Å (O2–N4); 1.285(1) Å (O3–N5); 1.294(1) Å (O4–N6) for **2** and 1.279(3) Å (N2–O1); 1.276(4) Å (N3–O2) for **1**. The bond angles are $126.1(3)^\circ$ (O2–N3–C12) and $126.2(3)^\circ$ (O1–N2–C12) for **1** and $127.2(8)^\circ$ (O1–N3–C13); $124.4(8)^\circ$ (O2–N4–C13); $124.2(9)^\circ$ (O3–N5–C28); $125.8(1)^\circ$ (O4–N6–C28) for **2**. The C=C lengths are 1.195(5) Å (C5–C4) for **1** and 1.193(1) Å (C6–C5) and 1.201(1) Å (C20–C21) for **2**.

Theoretical Calculations. Semiempirical (AM1) calculations with extended configuration interaction (CI) were performed for the biradicals **1**, **2**, and **T** (the analogue of **1** and **2** with three benzene rings in the spacer). The singlet–triplet splitting (ΔE_{ST}) and the spin densities were determined. The influence of structure alternation on the magnitude of ΔE_{ST} was estimated as well.

TABLE 1. Singlet–Triplet splitting (ΔE_{ST}) Calculated with ROHF/AM1/CAS (8,8)^a

molecule geometry	1	2	T
$\theta_1 = \theta_2 = \theta_3 = 0^\circ$	3.6160	2.8524	3.7943
$\theta_1 = 0^\circ, \theta_2 = 21^\circ, \theta_3 = 3^\circ$	3.2638	2.4690	3.1781
$\theta_1 = 20^\circ, \theta_2 = \theta_3 = 0^\circ$	4.1582	3.3262	4.5220
$\theta_1 = 20^\circ, \theta_2 = 21^\circ, \theta_3 = 3^\circ$	1.4007	0.9369	1.2700

^a The values are in kJ/mol.

TABLE 2. Heats of formation calculated with ROHF/AM1/CAS (8,8)^a

molecule geometry	1	2	T
$\theta_1 = \theta_2 = \theta_3 = 0^\circ$	1227.611	1262.359	1187.645
$\theta_1 = 0^\circ, \theta_2 = 21^\circ, \theta_3 = 3^\circ$	1252.284	1292.634	1210.456
$\theta_1 = 20^\circ, \theta_2 = \theta_3 = 0^\circ$	1232.322	1267.827	1191.888
$\theta_1 = 20^\circ, \theta_2 = 21^\circ, \theta_3 = 3^\circ$	1224.602	1259.351	1184.900

^a The values are in kJ/mol.

The geometry of the biradicals were optimized with inclusion of 6 frontier MOs occupied by 6 electrons in the active space of the CI. Two minima of **T** with close energy were detected (see Table 2): one corresponding to a planar structure ($\theta_1 = \theta_2 = \theta_3 = 0^\circ$, see Figure 9) separated by ~ 2.7 kJ/mol from a molecule with $\theta_1 = 20^\circ$, $\theta_2 = 21^\circ$, and $\theta_3 = 3^\circ$. Substitution of one carbon atom in the central benzene ring with nitrogen led to a slightly larger difference between the energies of the planar form (~ 3 kJ/mol) as compared to the respective twisted conformation. To determine more accurately ΔE_{ST} , single-point energy calculations of the optimized structures with extended CI were made. The correlation included configurations resulting from the mixing of 8 electrons in 8 MOs (or CAS(8,8)). The effect of the out-of-plane rotation

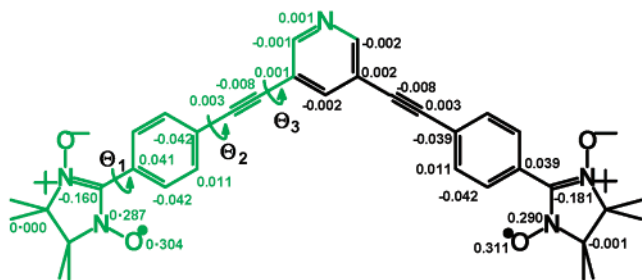


FIGURE 9. Spin density distribution of biradicals **1** (green) and **T** (black) calculated with ROHF/AM1/CIS (20,20).

on the magnitude of the singlet–triplet splitting was estimated by consideration of two intermediate structures, one with $\theta_1 = 20^\circ$ and $\theta_2 = \theta_3 = 0^\circ$ and the other with $\theta_1 = 0^\circ$, $\theta_2 = 21^\circ$ and $\theta_3 = 3^\circ$. For comparison the X-ray results for the dihedral angles of **1** were found with ($\theta_1 = 21^\circ$, $\theta_2 = 2.4^\circ$, and $\theta_3 = 5.7^\circ$). The results for ΔE_{ST} are summarized in Table 1, while the heats of formation of all molecules are given in Table 2.

All values in Table 1 are positive, which means that all biradicals have a triplet ground state, in accordance with the topological predictions. It can be seen, that the replacement of the central benzene ring from the pyridine has a moderate effect on the exchange interaction. The 3,5-substituted pyridine is comparable to benzene as a coupling unit. The 2,6-substituted biradical features slightly smaller singlet–triplet gap but the triplet is still well below the singlet. The variation of the singlet–triplet splitting can be explained in terms of MOs involved in the interaction. A scheme of the frontier MOs of **1** included in the active space is shown in Figure 10. The same MO pattern was preserved in the other two radicals as well.

Substitution of carbon with nitrogen at position 1 or 4 in the central ring of the coupler constitutes the only structural difference between the three biradicals, which should be reflected in the exchange interaction. From all depicted MOs, only two have non-zero coefficients on one of these atomic sites, namely HOMO – 1 and LUMO + 1. Moreover, the value in position 4 is much larger than that in 1. Therefore, the 3,5-substitution of pyridine in **1** practically does not alter the singlet–triplet separation. On the other hand, the 2,6-pattern in **2** results in MOs with nitrogen contribution. This could be responsible for the slight decrease of ΔE_{ST} . The largest ΔE_{ST} is obtained when the bridging π -system is planar. This is an indication that the high-spin ground state is stabilized by the spin-polarization through the bridge.

Good illustrations of this phenomenon are the calculated spin densities. The values for the structures with largest ΔE_{ST} of **1** (green) and **T** (black) are shown in the Figure 9.

It can be seen that (1) there is sign alternation throughout the molecules, characteristic of the ferromagnetic coupling of the unpaired electrons, and (2) introduction of nitrogen affects only the energy of the system but does not change the spin density distribution.

Thus, nitrogen can be considered as suitable replacement of carbon in the coupling unit, sustaining the triplet ground state and furthermore offering ligation advantages.

Conclusions

In this paper, we demonstrate that two NIT attached to phenylethynyl spacer, which are linked (meta-type) at both ends of 3,5- and 2,6-pyridines by ~ 1.5 nm distance (X-ray) are intramolecularly exchange coupled (**1** and **2**) with $J \gg h\nu$. Biradicals **1** and **2** have approximately the same zero-field splitting values independent of the position of the pyridyl nitrogen. In both molecules **1** and **2**, the position of the pyridyl nitrogen has no influence on the molecular ground state as evidenced by cryogenic EPR measurements, where both exhibit Curie like behavior. These experimental findings point toward triplet ground state or its near-degeneracy with a singlet state while the theoretical calculations support the triplet entities. In addition to EPR, the extinction coefficient of the $n-\pi^*$ transition of the UV–vis spectra in the visible region can also be used to estimate roughly the number radical units in a molecule. This approach can be used to distinguish a monoradical from a biradical or even a triradical. The preparation of the extended metal complexes of **1** and **2** are underway.

Experimental Section

3,5-Bis(4-formylphenylethynyl)pyridine (9). Twenty milliliters of triethylamine and 20 mL of THF were frozen in a Schlenk flask using liquid nitrogen, and 0.94 g (4 mmol) of 3,5-dibromopyridine, 0.141 g (0.2 mmol) of $\text{Pd}(\text{PPh}_3)_2\text{Cl}_2$, 1.3 g (10 mmol) of **8**, and 0.0762 g (0.4 mmol) of CuI were added into the flask under argon over flow and deaerated by freeze–pump–thaw cycles five times. The brown mixture was refluxed at 60°C for 4 days. After evaporation of the solvents the crude product was extracted with dichloromethane and evaporated to brownish yellow powder. In TLC (CHCl_3) the first spot from the top was dimer ($R_f \sim 0.75$) **8** [m/z 258.0 (100%)], the second spot was monocoupled product ($R_f \sim 0.5$) **10**, yield 0.550 g (54%), and the third one was the desired dialdehyde ($R_f \sim 0.2$) **9**. The fractions were separated by column chromatography (CHCl_3) to get yellowish mono coupled aldehyde and the desired yellow dialdehyde. Yield: 0.335 g (27%). $^1\text{H NMR}$ (250 MHz, CDCl_3 , RT) δ : 10 (s, 2H), 9.7 (s, 2H), 7.95 (s, 1H), 7.89 (d, 4H, $^3J = 8.21$ Hz), 7.69 (d, 4H, $^3J = 8.22$ Hz). $^{13}\text{C NMR}$ (62.5 MHz, CDCl_3 , RT) δ : 191.3, 151.4, 140.9, 136.0, 132.3, 129.7, 128.3, 119.6, 92.4, 88.7. FD MS (70 eV): m/z 335.0 (100). UV (toluene, $c = 10^{-4}$ M): 305 nm ($\epsilon = 32\ 613\ \text{M}^{-1}\ \text{cm}^{-1}$). FTIR (KBr disk; ν in cm^{-1}): 3030 (s, Py–C–H), 2754 and 2856 (w, C–H, carbonyl), 1685 (vs, C=O), 825 (vs, aromatic CH out of plane deformation). Mp: $185\text{--}187^\circ\text{C}$ (decomposed before melting).

4-(5-Bromopyridin-3-ylethynyl)benzaldehyde (10). $^1\text{H NMR}$ (250 MHz, CDCl_3 , RT) δ : 10.02 (s, 1H), 8.68 (s, 1H), 8.64 (d, 1H, $^4J = 1.9$ Hz), 7.99 (s, 1H), 7.89 (d, 2H, $^3J = 8.21$ Hz), 7.38 (d, 2H, $^3J = 7.9$ Hz). $^{13}\text{C NMR}$ (62.5 MHz, $\text{DMSO}-d_6$, RT) δ : 191.98, 149.9, 140.4, 135.5, 131.8, 129.2, 126.5, 120.0, 92.1, 87.5. FD MS (70 eV): m/z 285.2 (~ 89) and 287.2 (100). FTIR (KBr disk; ν in cm^{-1}): 3012 (w, Py CH stretching), 1680 (vs, C=O), 829 (s, aromatic CH out of plane deformation). Mp: $150\text{--}152^\circ\text{C}$.

4-(5-Bromopyridin-3-ylethynyl)-1-(1,3-dihydroxy-4,4,5,5-tetramethylimidazolin-2-yl)benzene (14). A 0.200 g (0.7 mmol) portion of **10** was taken in 10 mL each of toluene and methanol with 0.120 g (0.8 mmol) of 2,3-dimethyl-2,3-bis-(hydroxyamino)butane¹⁸ and refluxed at 90°C for 3 days under argon bubbling. The formed turbid yellow solution was filtered, and the condensation product **14** was obtained as yellow

(18) (a) Ovcharenko, V. I.; Fokin, S. V.; Romanenko, G. V.; Korobkov, I. V.; Rey, P. *Russ. Chem. Bull.* **1999**, *48*, 1519–1525. (b) Ovcharenko, V. I.; Fokin, S. V.; Rey, P. *Mol. Cryst. Liq. Cryst.* **1999**, *334*, 109–119.

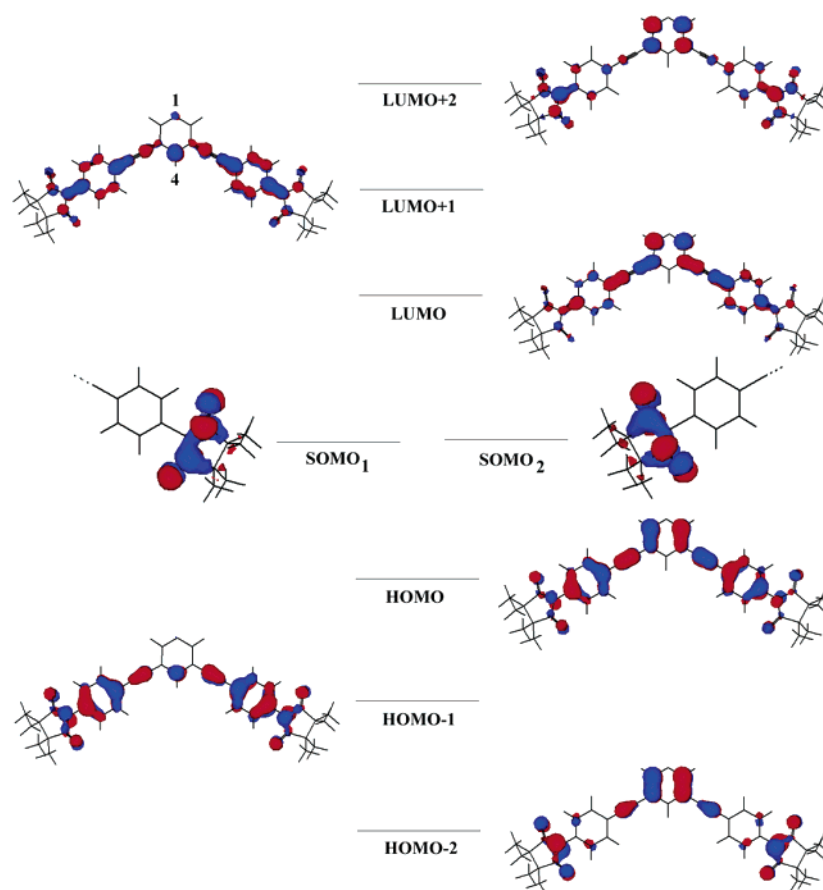


FIGURE 10. ROHF/AM1-calculated frontier MOs of biradical **1**; pictured with contour value of 0.035 and 64×64 grid points.

powder. Yield: 0.134 g (46%). $^1\text{H NMR}$ (250 MHz, $\text{DMSO-}d_6$, RT) δ : 8.73 (s, 1H), 8.72 (s, 1H), 8.3 (s, 1H), 7.55 (s), 7.23 (d, 2H), 7.16 (d, 2H), 4.54 (s, 1H), 1.08, 1.04. $^{13}\text{C NMR}$ (62.5 MHz, $\text{DMSO-}d_6$, RT) δ : 150.1 and 149.7, 143.8, 140.6, 131.0, 128.9, 128.2, 120.1, 120.0, 94.0, 89.9, 84.4, 66.3, 24.4 and 17.2.

4-(5-Bromopyridin-3-ylethynyl)-1-(1-oxyl-3-oxo-4,4,5,5-tetramethylimidazolin-2-yl)benzene (3). A 0.130 g (0.313 mmol) portion of **14** was taken with 0.069 g (0.32 mmol) of NaIO_4 in 25 mL each of chloroform and water. The solution was stirred for 20 min in an ice-cold bath. The formed blue organic layer was separated and dried over MgSO_4 and evaporated to yellow powder. The radical **3** was obtained as blue crystalline powder after column chromatography on silica gel (1:2 acetone/petroleum ether boiling range $30\text{--}40^\circ\text{C}$; $R_f \sim 0.74$). Yield: 26 mg (20%). EPR (in toluene 10^{-3} M; RT; $\nu = 9.397562$ GHz; 2.01 mW power; 2 scans): Five lines, $g_{\text{iso}} = 2.0067$, $a_{\text{N}}/2 = 3.65$ G. UV/vis (toluene $c = 10^{-5}$ M): 389 nm ($\epsilon = 9474 \text{ M}^{-1} \text{ cm}^{-1}$), 620 nm ($\epsilon = 252 \text{ M}^{-1} \text{ cm}^{-1}$). FTIR (KBr disk; ν in cm^{-1}): 1354 (s, N–O). Mp: $167\text{--}169^\circ\text{C}$.

3,5-Bis[4-(1,3-dihydroxy-4,4,5,5-tetramethylimidazolin-2-yl)phenylethynyl]pyridine (13). A 0.154 g (0.456 mmol) portion of **9** was dissolved in methanol and dichloromethane 15 mL each. After addition of 0.225 g (1.5 mmol) of 2,3-dimethyl-2,3-bis(hydroxylamino)butane, the clear yellow solution was refluxed under argon bubbling at 60°C for 12 h. The light yellow precipitate of **13** was filtered and washed with chloroform and methanol, respectively. Yield: 0.100 g (37%). Compound **13** was used for the next step without purification and characterization.

3,5-Bis[4-(1-oxyl-3-oxo-4,4,5,5-tetramethylimidazolin-2-yl)phenylethynyl]pyridine (1). A 0.1 g (0.168 mmol) portion of **13** was taken with the phase-transfer solution of 10 mL each of chloroform and water. A 0.1 g (0.465 mmol) portion of NaIO_4 was added into the solution and stirred for

10 min. The blue organic layer was separated, and the aqueous layer was extracted with chloroform repeatedly, and the combined organic layers were concentrated into deep blue solution at 45°C under 75 mbar and purified by preparative chromatography (1:1 acetone/hexane) to afford **1** as blue powder. Yield: 35 mg (35%). EPR (in toluene 10^{-3} M, RT, $\nu = 9.405596$ GHz, 2.01 mW power, 2 Scans): nine lines, $g_{\text{iso}} = 2.0067$, $a_{\text{N}}/2 = 3.65$ G. UV/vis (toluene $c = 10^{-5}$ M): 617 nm ($\epsilon = 470 \text{ M}^{-1} \text{ cm}^{-1}$), 387 nm ($\epsilon = 15972 \text{ M}^{-1} \text{ cm}^{-1}$). FTIR (KBr disk; ν in cm^{-1}): 1390 (s, N–O). Anal. Calcd for $\text{C}_{35}\text{H}_{35}\text{N}_5\text{O}_4$: C, 71.29; H, 5.98; N, 11.88. Found: C, 70.28; H, 6.20; N, 11.49.

2,6-Bis(4-formylphenylethynyl)pyridine (11). A 20 mL portion of triethylamine and 20 mL of THF were frozen in a dry Schlenk flask using liquid nitrogen, and 0.94 g (4.0 mmol) of 2,6-dibromopyridine, 0.067 g (0.095 mmol) of $\text{Pd}(\text{PPh}_3)_2\text{Cl}_2$, 1.3 g (10 mmol) of **8**, and 0.0381 g (0.2 mmol) of CuI were added into the flask under argon over flow and deaerated using Schlenk line by freeze–pump–thaw cycles 5 times. The brown mixture was refluxed with stirring at 60°C for 3 days under argon. The solvents from the crude reaction mixture were evaporated and extracted with dichloromethane and evaporated to a brownish yellow powder. TLC (CH_2Cl_2): the first spot from the top was monocoupled [m/z 285.2 and 287.1 (100)] and the second was the desired dialdehyde **11**. The fractions were separated by column chromatography (CH_2Cl_2) to get yellowish dialdehyde. Yield: 0.8 g (60%). $^1\text{H NMR}$ (250 MHz, CDCl_3 , RT) δ : 10.02 (s, 2 H), 7.88 (d, 4 H, $^3J = 8.53$ Hz), 7.74 (m, 5 H, the pyridine $\text{C}_4\text{--H}$ and benzene protons also appears at the same ppm), 7.54 (d, 2 H, $^3J = 7.58$ Hz). $^{13}\text{C NMR}$ (62.5 MHz, CDCl_3 , RT) δ : 191.3, 143.4, 136.8, 136.1, 132.6, 129.6, 128.1, 127, 91.4, 88.5. FD MS (70 eV): m/z 335.3 (100). UV (toluene, $c = 10^{-4}$ M): 338 nm ($\epsilon = 28841 \text{ M}^{-1} \text{ cm}^{-1}$). FTIR (KBr disk; ν in cm^{-1}): 3051 (w, Py–C–H), 2850 and 2736 (w, carbonyl C–H), 2210 (m, C=C), 1697 (vs, C=O), 1601 (vs,

aromatic C=C), 1558 (vs, aromatic C=N). Mp: 192–194 °C (decomposed before melting).

2,6-Bis[4-(1,3-dihydroxy-4,4,5,5-tetramethylimidazolin-2-yl)phenylethynyl]pyridine (12). As described for the synthesis of **13**, 0.2 g (0.597 mmol) of **11** were dissolved in 10 mL of toluene and 5 mL of methanol, and after addition of 0.225 g (1.5 mmol) of 2,3-dimethyl-2,3-bis(hydroxylamino)butane the turbid yellow solution was heated under argon bubbling to 80 °C to get a clear solution and then refluxed for 2 days. The formed yellow precipitate of **12** was filtered and washed with chloroform and methanol, respectively. Yield: 0.215 g (61%). ¹H NMR (500 MHz, DMSO-*d*₆, RT) δ: 7.89 (t, 1 H, ³*J* = 8.01 Hz and ³*J* = 7.78 Hz), 7.81 (s), 7.64 (d, 2H, ³*J* = 7.86 Hz), 7.60 (d, 4 H, ³*J* = 7.93 Hz), 7.58 (d, 4 H, ³*J* = 7.99 Hz), 4.55 (s, 2 H), 1.08 (s, 12 H) and 1.04 (s, 12 H).

2,6-Bis[4-(1-oxo-3-oxo-4,4,5,5-tetramethylimidazolin-2-yl)phenylethynyl]pyridine (2). A 0.15 g (0.252 mmol) portion of **12** was taken in a phase-transfer solution of 15 mL each of chloroform and water. A 0.15 g (0.698 mmol) portion of NaIO₄ was added into the solution and stirred for 10 min. The blue organic layer was extracted with chloroform and concentrated into deep blue solution at 45 °C under 75 mbar and purified by preparative chromatography (1:1 acetone/hexane) to blue powder (**2**). Yield: 50 mg (34%). EPR (in toluene *c* = 10⁻³ M, RT, *ν* = 9.405379 GHz, 2.01 mW

power, 2 scans): nine lines, *g*_{iso} = 2.0067, *a*_N/2 = 3.65 G. UV/Vis (in toluene *c* = 10⁻⁵ M): 629 nm (*ε* = 499 M⁻¹ cm⁻¹), 387 nm (*ε* = 19 146 M⁻¹ cm⁻¹). FTIR (KBr disk; *ν* in cm⁻¹): 1365 (s, N–O).

Acknowledgment. C.R. and M.B. gratefully acknowledge the Graduate College, TU- Darmstadt for the Ph.D. fellowship. We thank Giorgio Zoppellaro (MPI Polymer Research, Mainz) and Dr. Sergei Fokin and Prof. Dr. Victor Ovcharenko, International Tomography Center, Russian Academy of Sciences, Novosibirsk, Russia, for many helpful discussions. A.I. kindly acknowledges the support given by the Marie Curie program. M.B. also thanks the DFG for its continuous support.

Supporting Information Available: General details and synthetic procedure toward compounds **4** and **5**. ESR spectra ($\Delta m_s = \pm 1$) of **1** and **2** at various temperatures. X-ray crystallographic data and experimental parameters of **1** and **2**. This material is available free of charge via the Internet at <http://pubs.acs.org>.

JO034597N